Inorganic Chemistry

Article

pubs.acs.org/IC

Mechanistic Borderline of One-Step Hydrogen Atom Transfer versus Stepwise Sc^{3+}-Coupled Electron Transfer from Benzyl Alcohol Derivatives to a Non-Heme Iron(IV)-Oxo Complex

Yuma Morimoto,[†] Jiyun Park,[†] Tomoyoshi Suenobu,[†] Yong-Min Lee,[‡] Wonwoo Nam,*[,‡] and Shunichi Fukuzumi*[,†,‡]

[†]Department of Material and Life Science, Graduate School of Engineering, Osaka University, ALCA, Japan Science and Technology Agency (JST), Suita, Osaka 565-0871, Japan

[‡]Department of Bioinspired Science, Ewha Womans University, Seoul 120-750, Korea

Supporting Information

ABSTRACT: The rate of oxidation of 2,5-dimethoxybenzyl alcohol (2,5-$(MeO)_2C_6H_3CH_2OH$) by $[Fe^{IV}(O)(N4Py)]^{2+}$ (N4Py = *N*,*N*-bis(2-pyridylmethyl)-*N*-bis(2-pyridyl)-methylamine) was enhanced significantly in the presence of $Sc(OTf)_3$ (OTf^- = trifluoromethanesulfonate) in acetonitrile (e.g., 120-fold acceleration in the presence of Sc^{3+}). Such a remarkable enhancement of the reactivity of $[Fe^{IV}(O)(N4Py)]^{2+}$ in the presence of Sc^{3+} was accompanied by the disappearance of a kinetic deuterium isotope effect. The radical cation of 2,5-$(MeO)_2C_6H_3CH_2OH$ was detected in the course of the reaction in the presence of Sc^{3+}. The dimerized alcohol and aldehyde were also produced in addition to the monomer aldehyde in the presence of Sc^{3+}. These results indicate that the reaction mechanism is changed from one-step hydrogen atom transfer (HAT) from 2,5-$(MeO)_2C_6H_3CH_2OH$ to $[Fe^{IV}(O)(N4Py)]^{2+}$ in the absence of Sc^{3+} to stepwise Sc^{3+}-coupled electron transfer, followed by proton transfer in the presence of Sc^{3+}. In contrast, neither acceleration of the rate nor the disappearance of the kinetic deuterium isotope effect was observed in the oxidation of benzyl alcohol ($C_6H_5CH_2OH$) by $[Fe^{IV}(O)(N4Py)]^{2+}$ in the presence of $Sc(OTf)_3$. Moreover, the rate constants determined in the oxidation of various benzyl alcohol derivatives by $[Fe^{IV}(O)(N4Py)]^{2+}$ in the presence of $Sc(OTf)_3$ (10 mM) were compared with those of Sc^{3+}-coupled electron transfer from one-electron reductants to $[Fe^{IV}(O)(N4Py)]^{2+}$ at the same driving force of electron transfer. This comparison revealed that the borderline of the change in the mechanism from HAT to stepwise Sc^{3+}-coupled electron transfer and proton transfer is dependent on the one-electron oxidation potential of benzyl alcohol derivatives (ca. 1.7 V vs SCE).

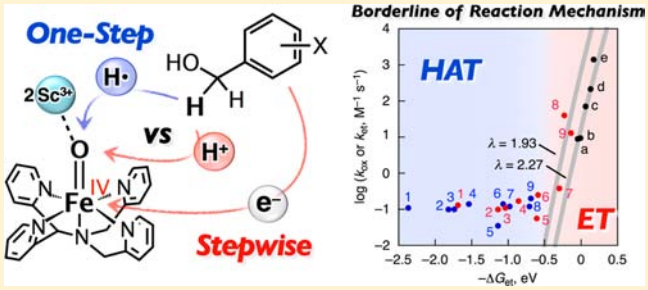

INTRODUCTION

Homolytic C−H bond cleavage of organic compounds is one of the fundamental reaction steps in various types of oxidation processes both in synthetic and biological chemistry.[1] Laboratory-scale syntheses and industrial oxidation processes have utilized metal-oxo reagents (e.g., $KMnO_4$) and a metal oxide surface for the oxidation of organic substrates.[2,3] In the oxidative enzymes, heme and nonheme iron oxygenases represented by cytochrome P450 and taurine/α-ketoglutarate dioxygenase (TauD), respectively, high-valent iron-oxo species have been regarded as reactive intermediates in their catalytic cycles, where C−H bond is cleaved by oxometal species (M═O) and O−H bond is formed in the process of hydrogen atom transfer (HAT) from substrate to oxometal species.[4−6] In the enzymatic oxidation reactions, for example, hydroxylation, oxidation of alcohols, desaturation, cyclization, and chlorination, the initial step of those processes is widely believed to be activation of C−H bonds via HAT from a substrate to high-valent iron-oxo species.[4−10]

In general, there are three possible reaction pathways in HAT reactions of iron-oxo species (Fe^{IV}=O), as shown in Scheme 1. Since a hydrogen atom consists of an electron and a proton, the proposed mechanisms are (1) stepwise proton transfer followed by electron transfer (PT/ET), (2) stepwise electron transfer followed by proton transfer (ET/PT), and (3) one-step HAT, in which an electron and a proton are transferred in a concerted manner. In the case of iron-oxo species, one-step

Scheme 1. Three Possible Reaction Pathways in HAT Reactions of Iron-Oxo Species

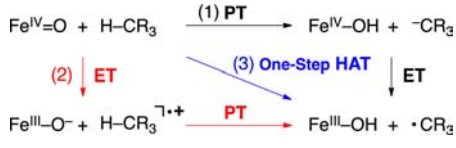

Received: July 30, 2012
Published: September 6, 2012

   dx.doi.org/10.1021/ic3016723 | *Inorg. Chem.* 2012, 51, 10025−10036

HAT can be generally regarded as concerted proton−electron transfer (CPET), because an electron and a proton are transferred simultaneously to the metal center and the oxo moiety, respectively.[11] Tremendous efforts have so far been devoted to elucidate the mechanism of HAT reactions of iron-oxo species by employing model complexes bearing heme and nonheme ligands in the field of bioinorganic chemistry, where the transfer of an electron and a proton proceeds in a concerted maner.[11−19] There are some cases where C−H bond activation by iron-oxo species undergoes via an ET/PT pathway when electron-rich substrates such as *N*,*N*-dimethylaniline derivatives are used as substrates.[20] In the case of HAT reactions from substrates to triplet excited states of photosensitizers, the mechanistic borderline of one-step HAT vs ET/PT pathways has been clarified by changing the electron donor ability of hydrogen donors as well as the electron acceptor ability of hydrogen acceptors.[21] The borderline of one-step hydride-transfer vs ET/PT pathways has also been discussed for Sc^{3+}-promoted hydride transfer from an NADH analogue to a *p*-benzoquinone derivative.[22,23] There are also studies on the mechanistic change from one-step HAT to ET/PT with metal-centered oxidants.[24,25] However, the mechanistic borderline of one-step HAT vs ET/PT pathways in C−H bond cleavage by iron-oxo species has yet to be clarified because of the lack of systematic studies.

We report herein one example of the switch of the reaction pathway from a one-step HAT pathway in C−H bond activation of benzyl alcohol derivatives ($X\text{-}C_6H_4CH_2OH$) with a nonheme iron(IV)-oxo complex, $[Fe^{IV}(O)(N4Py)]^{2+}$ (N4Py = *N*,*N*-bis(2-pyridylmethyl)-*N*-bis(2-pyridyl)-methylamine),[15,16] to a stepwise ET/PT pathway by addition of Sc^{3+}. We have recently reported that one-electron reduction of $[Fe^{IV}(O)(N4Py)]^{2+}$ is accelerated by the addition of Lewis acids such as Ca^{2+}, Mg^{2+}, and Zn^{2+}, and so forth.[26,27] Electron-acceptability of $[Fe^{IV}(O)(N4Py)]$ is enhanced by the much stronger binding of Sc^{3+} to $[Fe^{III}(O)(N4Py)]$ than $[Fe^{IV}(O)(N4Py)]$. We have chosen Sc^{3+} in this work, because Sc^{3+} has the largest acceleration effect among examined metal ions. In the presence of 10 mM of Sc^{3+}, the reduction potential of the iron(IV)-oxo complex (E_{red}) was shifted from 0.51 V vs SCE to the positive direction up to 1.19 V.[26−30] Such a change in the E_{red} value of $[Fe^{IV}(O)(N4Py)]^{2+}$ by the presence of Sc^{3+} and well-determined reduction potential provides an excellent opportunity to scrutinize the borderline of one-step HAT vs ET followed by subsequent PT steps in C−H bond activation by metal-oxo species in a systematic manner.

EXPERIMENTAL SECTION

Materials. Benzyl alcohol ($C_6H_5CH_2OH$), pentamethylbenzyl alcohol ($Me_5C_6CH_2OH$), 2,5-dimethoxybenzyl alcohol (2,5-$(MeO)_2C_6H_3CH_2OH$), 2,5-dimethoxybenzoic acid, and scandium(III) trifluoromethanesulfonate ($Sc(OTf)_3$) were purchased from Aldrich Chemicals Co. *p*-Chlorobenzyl alcohol (*p*-$ClC_6H_4CH_2OH$), *p*-methylbenzyl alcohol (*p*-$MeC_6H_4CH_2OH$), 3,5-dimethoxybenzyl alcohol (3,5-$(MeO)_2C_6H_3CH_2OH$), 3,4,5-trimethoxybenzyl alcohol (3,4,5-$(MeO)_3C_6H_2CH_2OH$), and benzoic acid were obtained from Tokyo Chemical Industry Co., Ltd.; *p*-nitrobenzyl alcohol (*p*-$NO_2C_6H_4CH_2OH$) and *p*-methoxybenzyl alcohol (*p*-$MeOC_6H_4CH_2OH$) were obtained from Wako Pure Chemical Industries, Ltd. and lithium aluminum deuteride ($LiAlD_4$) was purchased from CIL, Inc. The commercially available compounds used in this study were the best available purity and used without further purification unless otherwise noted. Acetonitrile (MeCN) was dried according to the literature procedures and distilled under Ar prior to use.[31] Iodosylbenzene (PhIO) was prepared by a literature method.[32] Nonheme iron(II) complex, $[Fe(N4Py)](ClO_4)_2$ (N4Py = *N*,*N*-bis(2-pyridylmethyl)-*N*-bis(2-pyridyl)methylamine), and its iron(IV)-oxo complex, $[Fe^{IV}(O)(N4Py)]^{2+}$, were prepared according to the literature methods.[15,16] For example, $[Fe^{IV}(O)(N4Py)]^{2+}$ was prepared by reacting $[Fe(N4Py)](ClO_4)_2$ (5.0 mM) with 1.2 equiv of PhIO (6.0 mM) in MeCN at ambient temperature. The deuterated compounds, phenyl [$^2H_2$]methanol ($C_6H_5CD_2OH$) and 2,5-dimethoxyphenyl [$^2H_2$]methanol (2,5-$(MeO)_2C_6H_3CD_2OH$), were prepared by reduction of benzoic acid and 2,5-dimethoxybenzoic acid (2,5-$(MeO)_2C_6H_3COOH$) with $LiAlD_4$ in ether.[33]

Spectral and Kinetic Measurements. Reactions of benzyl alcohol and its derivatives with $[Fe^{IV}(O)(N4Py)]^{2+}$ (1.0×10^{-4} M) were examined by monitoring spectral changes in the presence of various concentrations of benzyl alcohol or its derivatives (1.0×10^{-3}−2.0×10^{-1} M) in the absence and presence of $Sc(OTf)_3$ in deaerated MeCN at 298 K using a Hewlett-Packard 8453 photodiode-array spectrophotometer and a quartz cuvette (path length =10 mm). Kinetic measurements for 2,5-$(MeO)_2C_6H_3CH_2OH$ in the presence of Sc^{3+} were performed on a UNISOKU RSP-601 stopped-flow spectrometer equipped with a MOS-type highly sensitive photodiode array or a Hewlett-Packard 8453 photodiode array spectrophotometer at 298 K. Rates of reactions of benzyl alcohol and its derivatives with $[Fe^{IV}(O)(N4Py)]^{2+}$ were monitored by a decrease in the absorption band due to $[Fe^{IV}(O)(N4Py)]^{2+}$ (λ_{max} = 695 nm) in the absence and presence of $Sc(OTf)_3$ in MeCN. The concentration of benzyl alcohol or its derivatives was maintained to be more than 10-fold excess of $[Fe^{IV}(O)(N4Py)]^{2+}$ to keep pseudo-first-order conditions. Pseudo-first-order rate constants were determined by a least-squares fit of the first-order plot of time course of spectral change. Reactions of 3,4,5-$(MeO)_3C_6H_2CH_2OH$ with $[Fe^{IV}(O)(N4Py)]^{2+}$ in the presence of Sc^{3+} were performed in the presence of 0.10 mM of $[Fe^{IV}(O)(N4Py)]^{2+}$, 0.050 mM of 3,4,5-$(MeO)_3C_6H_2CH_2OH$, and excess amount of Sc^{3+} (5.0−20 mM).

Electrochemical Measurements. Measurements of cyclic voltammetry (CV) and second harmonic AC voltammetry (SHACV) were performed at 298 K using a BAS 630B electrochemical analyzer in deaerated MeCN containing 0.10 M $TBAPF_6$ as a supporting electrolyte at 298 K. A conventional three-electrode cell was used with a platinum working electrode and a platinum wire as a counter electrode. The measured potentials were recorded with respect to $Ag/AgNO_3$ (1.0×10^{-2} M). The one-electron oxidation potential values (E_{ox}) (vs $Ag/AgNO_3$) were converted to those vs SCE by adding 0.29 V.[34] All electrochemical measurements were carried out under an Ar atmosphere.

EPR Measurements. Electron paramagnetic resonance (EPR) detection of iron(III) complexes and radical cation of 2,5-$(MeO)_2C_6H_3CH_2OH$ was performed as follows: Typically, a MeCN solution of $[Fe^{IV}(O)(N4Py)]^{2+}$ (1.0×10^{-3} M) in the absence and presence of $Sc(OTf)_3$ (1.0×10^{-2} M) in an EPR cell (3.0 mm i.d.) was purged with N_2 for 5 min. Then, deaerated benzyl alcohol or 2,5-$(MeO)_2C_6H_3CH_2OH$ solution (5.0×10^{-2} M) was added to the solution. The EPR spectra of the radical cation of 2,5-$(MeO)_2C_6H_3CH_2OH$ and iron(III) complexes were recorded on a JEOL JES-RE1XE spectrometer at 243 and 77 K, respectively. The magnitude of modulation was chosen to optimize the resolution and signal-to-noise (S/N) ratio of the observed spectra under non-saturating microwave power conditions. The *g* value was calibrated using an Mn^{2+} marker (*g* = 2.034, 1.981). Computer simulation of the EPR spectra was carried out by using Calleo EPR version 1.2 (Calleo Scientific Publisher) on a personal computer.

NMR Measurements. ^1H NMR spectra were recorded on a JEOL JMN-AL-300 NMR spectrometer at room temperature. To obtain clear NMR signal by removing inorganic products, reaction solutions with Sc^{3+} were treated with alumina column before measurement. The yields of the oxidation products were determined based on the peak of iodobenzene (between 7.0 and 8.0 ppm), which is a product of the reaction of $[Fe^{II}(N4Py)]^{2+}$ with iodosylbenzene to form $[Fe^{IV}(O)(N4Py)]^{2+}$.

dx.doi.org/10.1021/ic3016723 | *Inorg. Chem.* 2012, 51, 10025−10036

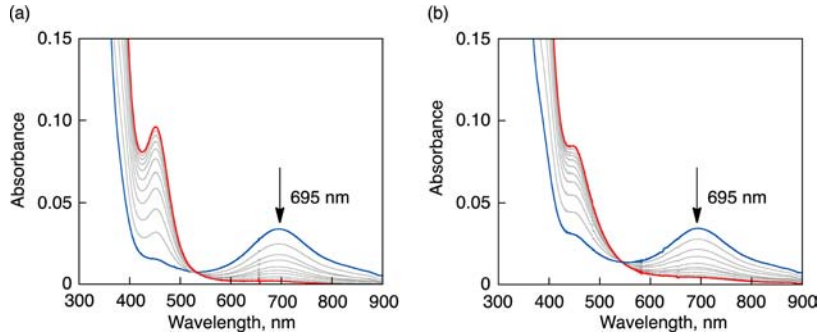

Figure 1. Spectral changes observed in the oxidation of benzyl alcohol (50 mM) by $[Fe^{IV}(O)(N4Py)]^{2+}$ (0.1 mM) in MeCN at 298 K in the absence (a) and presence (b) of Sc^{3+} (20 mM).

Calculations. Density functional theory (DFT) calculations on the properties of molecules were performed with the UB3LYP density-functional and the 6-311G++(d,p) basis set.[35] All calculations were performed using Gaussian 09, revision A.02.[36] Graphical outputs of the computational results were generated with the Gauss View software program (ver. 3.09) developed by Semichem, Inc.[37]

RESULTS AND DISCUSSION

Oxidation of Benzyl Alcohol by $[Fe^{IV}(O)(N4Py)]^{2+}$. Oxidation of benzyl alcohol by the iron(IV)-oxo complex was examined both in the absence and presence of Sc^{3+} at 298 K in MeCN. Addition of excess amount of benzyl alcohol (50 mM) to the solution of $[Fe^{IV}(O)(N4Py)]^{2+}$ (0.10 mM) caused the spectral change with a clean isosbestic point in both the absence and the presence of Sc^{3+} (20 mM) as shown in Figures 1a and 1b, respectively. The decay of the characteristic absorption band due to $[Fe^{IV}(O)(N4Py)]^{2+}$ (695 nm) was accelerated with increase in concentration of benzyl alcohol in both the absence and the presence of Sc^{3+} (Supporting Information, Figures S1a and S1b), obeying pseudo-first-order kinetics. The pseudo-first-order rate constants (k_{obs}) increased proportionally with an increase in concentration of benzyl alcohol, and the second-order rate constant (k_{ox}) was determined from the linear correlation to be 9.9×10^{-2} M^{-1} s^{-1} in the absence of Sc^{3+}, which was nearly the same as the value (1.1×10^{-1} M^{-1} s^{-1}) determined in the presence of Sc^{3+} (20 mM) as shown in Supporting Information, Figures S1c and S1d, respectively. In addition, the k_{obs} values were constant irrespective of the change in concentration of Sc^{3+} (Figure 2).

Product analysis of the oxidation of benzyl alcohol (1.0 mM) by $[Fe^{IV}(O)(N4Py)]^{2+}$ (1.0 mM) revealed the formation of benzaldehyde with 50% yield as a sole product both in the absence and presence of Sc^{3+} (10 mM) (Supporting Information, Figures S2a and S2b). The electrospray ionization mass spectrometry (ESI-MS) spectrum of the reaction solution performed in the absence of Sc^{3+} shows peaks at m/z 539.1 and 629.0, whose mass and isotope distribution indicate formation of $[Fe^{III}(OH)(N4Py)]^{2+}$ and $[Fe^{III}(OCH_2Ph)(N4Py)]^{2+}$, respectively (Supporting Information, Figures S3a and S3b). The formation of the iron(III) species was supported by taking EPR spectra of the reaction solution (Supporting Information, Figure S4a).[38] In the presence of Sc^{3+}, the ESI-MS spectrum of the resulting solution of the reaction shows peak at m/z 572.4, which indicates formation of $[Fe^{II}(N4Py)(OTf)]^{+}$ (calcd. m/z = 572.4) (Supporting Information, Figure S3c). The EPR spectrum, however, indicates that the major product of the reaction is not iron(II) but iron(III) species, $[Fe^{III}(N4Py)(NCMe)]^{3+}$ with orthogonal signals around g = 2.5 and 1.7 (Supporting Information, Figures S4b and S4c). The iron(III) complex might not be detected by ESI-MS probably because of the high one-electron-reduction potential of $[Fe^{III}(N4Py)(NCMe)]^{3+}$ (E_{red} = 1.0 V vs SCE) and the occurrence of the one-electron reduction from the iron(III) to iron(II) species under the ESI-MS condition.[39] To confirm the oxidation state of the iron complex in the resulting solution in both the absence and the presence of Sc^{3+}, a one-electron donor, ferrocene (Fc) was added into the solutions and one equiv of ferrocenium ion (Fc^{+}) to $[Fe^{IV}(O)(N4Py)]^{2+}$ was produced with the concurrent formation of $[Fe^{II}(N4Py)(NCMe)]$ in both cases (Supporting Information, Figures S5a and S5b). This indicates that $[Fe^{IV}(O)(N4Py)]^{2+}$ acts as a one-electron oxidant rather than a two-electron oxidant. It should be noted that the $[Fe^{III}(OH)(N4Py)]^{2+}$ produced during the reaction is not so reactive to oxidize $C_6H_5CHOH^{\bullet}$.

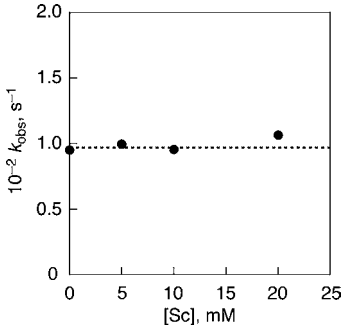

Figure 2. Dependence of the pseudo-first-order rate constant (k_{obs}) determined in the oxidation of $PhCH_2OH$ (1.0×10^{2} mM) by $[Fe^{IV}(O)(N4Py)]^{2+}$ (0.10 mM) on concentration of Sc^{3+}.

The rate of the oxidation of $PhCD_2OH$ in the presence of Sc^{3+} (20 mM) in MeCN is significantly slower than that of $PhCH_2OH$ as shown in Figure 3, giving a deuterium kinetic isotope effect (KIE) of 7.2 at 298 K.[40] As reported previously in the oxidation of benzyl alcohol by $[Fe^{IV}(O)(N4Py)]^{2+}$ in the absence of Sc^{3+},[17] such a large KIE value clearly indicates that the rate-determining step (r.d.s.) of the reaction is HAT from benzyl alcohol to $[Fe^{IV}(O)(N4Py)]^{2+}$ in both the absence and the presence of Sc^{3+}. The subsequent HAT from $C_6H_5CHOH^{\bullet}$ to $[Fe^{IV}(O)(N4Py)]^{2+}$ to yield C_6H_5CHO and $[Fe^{III}(OH)(N4Py)]^{2+}$ occurs with a much faster rate than the initial HAT because of the weaker C−H bond in the radical species.[41] This reaction mechanism is summarized in Scheme 2. In the presence of benzyl alcohol, $[Fe^{III}(OH)(N4Py)]^{2+}$ is converted to $[Fe^{III}(OCH_2C_6H_5)(N4Py)]^{2+}$ and H_2O. No acceleration of the initial HAT was observed in the presence of Sc^{3+}.

dx.doi.org/10.1021/ic3016723 | Inorg. Chem. 2012, 51, 10025−10036

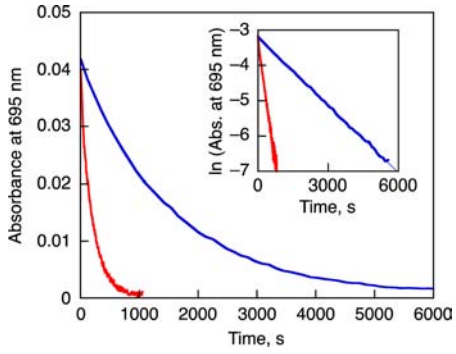

Figure 3. Time profiles of decay at 695 nm due to $[Fe^{IV}(O)(N4Py)]^{2+}$ (1.0 mM) in the oxidation of $PhCH_2OH$ (2.4×10^2 mM) (red) and $PhCD_2OH$ (2.4×10^2 mM) (blue) in the presence of Sc^{3+} (20 mM) in MeCN at 298 K. Inset shows the first-order plots of the spectral changes.

Scheme 2. Proposed Mechanism of Benzyl Alcohol Oxidation by $[Fe^{IV}(O)(N4Py)]^{2+}$

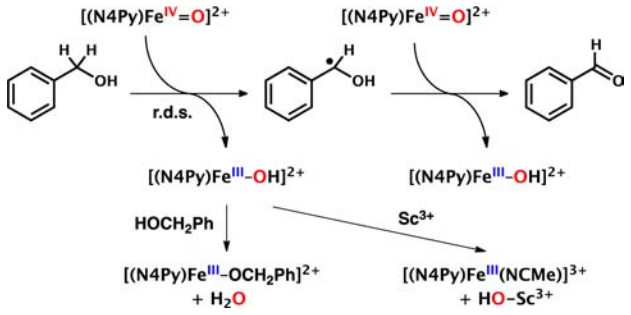

Oxidation of $2,5\text{-}(MeO)_2C_6H_3CH_2OH$ with $[Fe^{IV}(O)(N4Py)]^{2+}$. Different from the benzyl alcohol oxidation shown in Scheme 2, the rate of the oxidation of $2,5\text{-}(MeO)_2C_6H_3CH_2OH$ by $[Fe^{IV}(O)(N4Py)]^{2+}$ was significantly accelerated by the presence of Sc^{3+} (Figure 4b), as compared to the rate determined in the absence of Sc^{3+} (Figure 4a).

In the presence of Sc^{3+}, an intermediate with two absorption maxima at 430 and 455 nm appeared although it is not observed in the absence of Sc^{3+} (vide infra). The decay of the absorption band at 695 nm due to $[Fe^{IV}(O)(N4Py)]^{2+}$ in both the absence and the presence of Sc^{3+} obeyed first-order kinetics (Supporting Information, Figures S6a and S6c).[16] The pseudo-first order rate constant (k_{obs}) increased linearly with increasing concentration of $2,5\text{-}(MeO)_2C_6H_3CH_2OH$, and the second-order rate constant (k_{ox}) was determined by plotting k_{obs} vs $[2,5\text{-}(MeO)_2C_6H_3CH_2OH]$. The dependence of k_{ox} on $[Sc^{3+}]$ is shown in Figure 5 (red circles), where k_{obs} values increased with increasing concentration of Sc^{3+}, exhibiting both a first-order dependence and a second-order dependence on $[Sc^{3+}]$ as given by eq 1, where k_0 is the rate constant in the absence of Sc^{3+}, k_1 and k_2 are the rate constants exhibiting the first-order and second-order dependences on $[Sc^{3+}]$. The first-order and second-order dependence of k_{ox} on $[Sc^{3+}]$ is shown by a linear plot of $(k_{ox} - k_0)/[Sc^{3+}]$ vs $[Sc^{3+}]$ as shown in Supporting Information, Figure S7, where the intercept and the slope correspond to the contribution of the first-order and second-order dependence,

$$k_{ox} = k_0 + k_1[Sc^{3+}] + k_2[Sc^{3+}]^2 \quad (1)$$

respectively. Such a dependence of electron-transfer rate constants on $[Sc^{3+}]$ was reported previously for metal ion-coupled electron transfer from one-electron reductant to $[Fe^{IV}(O)(N4Py)]^{2+}$.[27] For instance, the dependence of second-order rate constant of electron transfer (k_{et}) from $[Fe^{II}(bpy)_3]^{2+}$ to $[Fe^{IV}(O)(N4Py)]^{2+}$ on $[Sc^{3+}]$ is shown in Figure 5 (black squares).

To determine the KIE value, the oxidation rate of a deuterated substrate ($2,5\text{-}(MeO)_2C_6H_3CD_2OH$) by $[Fe^{IV}(O)(N4Py)]^{2+}$ was also examined in both the absence and the presence of Sc^{3+}. In the absence of Sc^{3+}, the oxidation rate of $2,5\text{-}(MeO)_2C_6H_3CD_2OH$ (1.0×10^2 mM) by $[Fe^{IV}(O)(N4Py)]^{2+}$ (0.060 mM) was significantly slower than that of $2,5\text{-}(MeO)_2C_6H_3CH_2OH$ by $[Fe^{IV}(O)(N4Py)]^{2+}$ under the same conditions as employed in the oxidation of benzyl alcohol (Figure 6a). Second-order rate constants (k_H and k_D) were determined from the slopes of the plots of pseudo-first order rate constants of $2,5\text{-}(MeO)_2C_6H_3CH_2OH$ ($k_{H,obs}$) and $(2,5\text{-}(MeO)_2C_6H_3CD_2OH$ ($k_{D,obs}$) vs $[2,5\text{-}(MeO)_2C_6H_3CH_2OH]$ and $[2,5\text{-}(MeO)_2C_6H_3CD_2OH]$, respectively (red and blue circles in Figure 6c), respectively. The KIE value was determined to be 14 for the reaction performed at 298 K. This clearly indicates that HAT is the rate-determining step as the case of oxidation of benzyl alcohol by $[Fe^{IV}(O)(N4Py)]^{2+}$ in Scheme 2.[12b,16,42−45]

In sharp contrast to the case of the absence of Sc^{3+}, no KIE was observed in the presence of Sc^{3+} (Figures 6b and 6c). The disappearance of KIE by the presence of Sc^{3+} indicates a mechanistic change from HAT to a process in which C−H bond cleavage is not involved in the rate-determining step, which is most likely to be electron transfer (vide infra). Indeed, new transient absorption bands around 430 and 455 nm, which were not observed in the absence of Sc^{3+} in Figure 4a, were detected in the presence of Sc^{3+} (Figure 4b). These absorption bands agree with those observed in the one-electron oxidation of $2,5\text{-}(MeO)_2C_6H_3CH_2OH$ by a strong one-electron oxidant such as CAN, as shown in Figure 4b (green line).[46] This indicates the occurrence of electron transfer from $2,5\text{-}(MeO)_2C_6H_3CH_2OH$ to $[Fe^{IV}(O)(N4Py)]^{2+}$ to produce a radical cation of $2,5\text{-}(MeO)_2C_6H_3CH_2OH$ (i.e., $2,5\text{-}(MeO)_2C_6H_3CH_2OH^{\bullet+}$). The formation of the radical cation was confirmed by EPR measurements. Figure 7a shows an EPR spectrum of $2,5\text{-}(MeO)_2C_6H_3CH_2OH^{\bullet+}$ produced in the oxidation of $2,5\text{-}(MeO)_2C_6H_3CH_2OH$ by $[Fe^{IV}(O)(N4Py)]^{2+}$ in the presence of Sc^{3+}. The hyperfine coupling constants obtained in the computer simulation spectrum (Figure 7b) are in a reasonable agreement with those calculated by the DFT method (Figure 7c). The same EPR signal was observed in the one-electron oxidation of $2,5\text{-}(MeO)_2C_6H_3CH_2OH$ by $[Ru^{III}(bpy)_3]^{3+}$ (Supporting Information, Figure S7a).

The decay of the EPR signal of $2,5\text{-}(MeO)_2C_6H_3CH_2OH^{\bullet+}$ produced in the oxidation of $2,5\text{-}(MeO)_2C_6H_3CH_2OH$ by $[Fe^{IV}(O)(N4Py)]^{2+}$ in the presence of Sc^{3+} obeyed second-order kinetics (Figure 8a).[47] The second-order rate constant was determined to be $2.3 \times 10^3\ M^{-1}\ s^{-1}$ from the linear second-order plot (Figure 8b) and the initial concentration of $2,5\text{-}(MeO)_2C_6H_3CH_2OH$, which was determined by the double integration of the EPR spectrum by comparing with an authentic radical sample of 2,2-diphenyl-2-picrylhydrazyl (DPPH). The decay of the EPR signal of $2,5\text{-}(MeO)_2C_6H_3CH_2OH^{\bullet+}$ produced in the one-electron oxidation of $2,5\text{-}(MeO)_2C_6H_3CH_2OH$ by $[Ru^{III}(bpy)_3]^{3+}$ also obeyed second-order kinetics (Supporting Information, Figure S8b),

dx.doi.org/10.1021/ic3016723 | Inorg. Chem. 2012, 51, 10025−10036

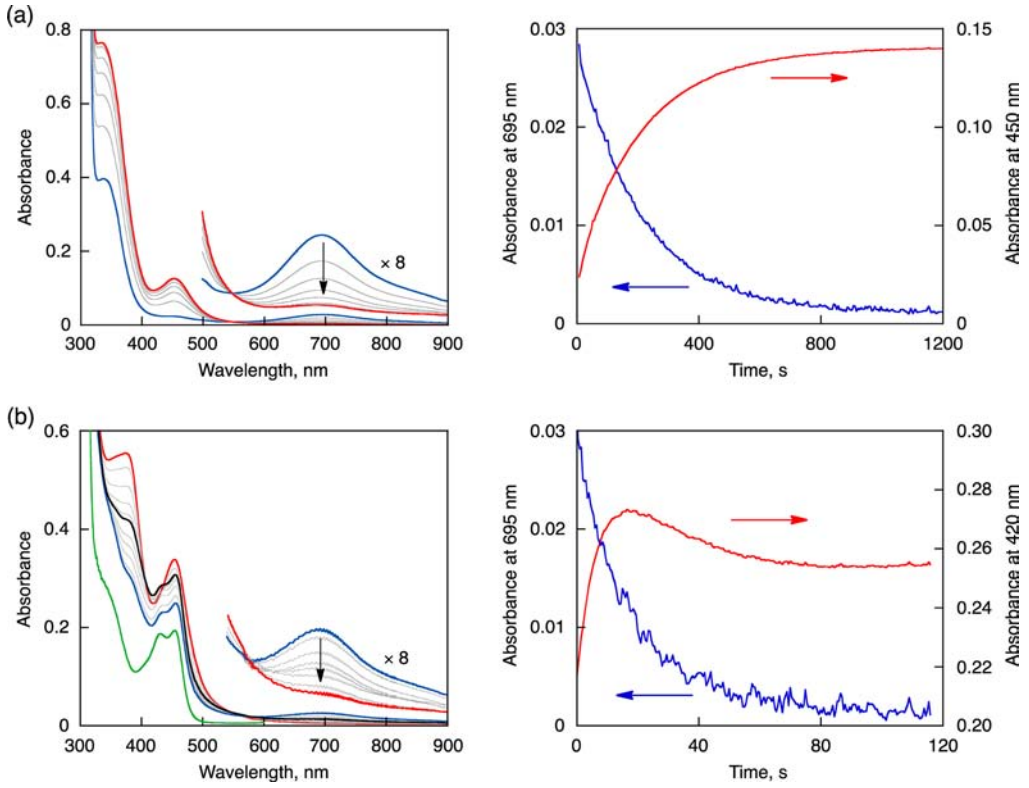

Figure 4. (a) Spectral changes observed in the oxidation of 2,5-$(MeO)_2C_6H_3CH_2OH$ (20 mM) by $[Fe^{IV}(O)(N4Py)]^{2+}$ (0.060 mM) in the absence of Sc^{3+} in deaerated MeCN. Right panel shows time courses monitored at 695 nm (blue) and 450 nm (red). (b) Spectral changes observed in the oxidation of 2,5-$(MeO)_2C_6H_3CH_2OH$ (2.5 mM) by $[Fe^{IV}(O)(N4Py)]^{2+}$ (0.060 mM) in the presence of Sc^{3+} (10 mM) (left panel; 4 s (blue), 30 s (black), and 120 s (red) after mixing) in deaerated MeCN. Green line indicates the reference spectrum of 2,5-$(MeO)_2C_6H_3CH_2OH$ radical cation produced by oxidizing 2,5-$(MeO)_2C_6H_3CH_2OH$ with $(NH_3)_2[Ce^{IV}(NO_3)_6]$ (CAN). Right panel shows time courses monitored at 695 nm (blue) and 420 nm due to 2,5-$(MeO)_2C_6H_3CH_2OH$ radical cation (red).

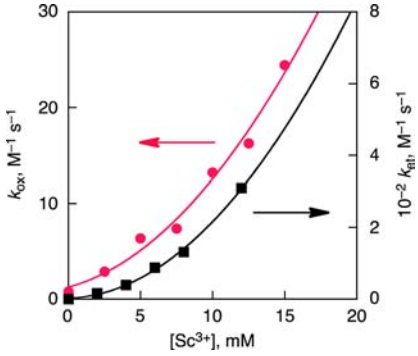

Figure 5. Plots of the second-order rate constant (k_{ox}) vs Sc^{3+} concentration in the oxidaiton of 2,5-$(MeO)_2C_6H_3CH_2OH$ by $[Fe^{IV}(O)(N4Py)]^{2+}$ (red circles) and the second-order rate constant (k_{et}) vs Sc^{3+} concentration in the Sc^{3+}-coupled ET from $[Fe(bpy)_3]^{2+}$ to $[Fe^{IV}(O)(N4Py)]^{2+}$ (black squares) in deaerated MeCN at 298 K.

indicating that bimolecular reactions of 2,5-$(MeO)_2C_6H_3CH_2OH^{\bullet+}$ are responsible for the decay of 2,5-$(MeO)_2C_6H_3CH_2OH^{\bullet+}$.

Product analyses of the oxidation of 2,5-$(MeO)_2C_6H_3CH_2OH$ by $[Fe^{IV}(O)(N4Py)]^{2+}$ in the absence and presence of Sc^{3+} were performed by the same method for the benzyl alcohol oxidation. ^1H NMR spectra of the reaction products obtained in the oxidation of 2,5-$(MeO)_2C_6H_3CH_2OH$ (1.0 mM) by one equiv of $[Fe^{IV}(O)(N4Py)]^{2+}$ (1.0 mM) in the absence of Sc^{3+} in CD_3CN revealed that 2,5-$(MeO)_2C_6H_3CH_2OH$ was converted to the corresponding aldehyde, 2,5-$(MeO)_2C_6H_3CHO$, with 50% yield as the case of benzyl alcohol oxidation (Supporting Information, Figure S9).[48] The major inorganic products were determined to be $[Fe^{III}(OH)(N4Py)]^{2+}$ and $[Fe^{III}(OCH_2C_6H_3(OMe)_2)(N4Py)]^{2+}$ by ESI-MS and EPR spectroscopy (Supporting Information, Figures S10 and S11). Titration of the resulting solution by Fc resulted in formation of Fc^+ with the same concentration as the initial concentration of $[Fe^{IV}(O)(N4Py)]^{2+}$ to produce $[Fe^{II}(N4Py)(NCMe)]^{2+}$ (Supporting Information, Figure S12). This indicates that $[Fe^{IV}(O)(N4Py)]^{2+}$ acts as a one-electron oxidant rather than two-electron oxidant in the oxidation of 2,5-$(MeO)_2C_6H_3CH_2OH$ as the case of $PhCH_2OH$ oxidation.

In the presence of Sc^{3+} (10 mM), however, the oxidation of 2,5-$(MeO)_2C_6H_3CH_2OH$ by $[Fe^{IV}(O)(N4Py)]^{2+}$ (1.0 mM) resulted in the oxidative coupling to yield 2,2′,5,5′-tetramethoxybiphenylyl-4,4′-dimethanol as a major product (31% yield, 0.31 mM) together with the further oxidized product 2,2′,5,5′-tetramethoxybiphenylyl-4,4′-dicarbaldehyde (1.0% yield, 0.010 mM) as well as the corresponding aldehyde (2,5-$(MeO)_2C_6H_3CHO$) only in 10% yield (0.10 mM) as shown in Scheme 3 with each products' yield and the oxidation equivalent (see Supporting Information, Figure S8b).[48] The ESI-MS and EPR spectrum of the resulting solution and titration of the resulting solution by Fc indicate that the inorganic products are iron(III) species and $[Fe^{IV}(O)(N4Py)]^{2+}$ acts as a one-electron oxidant in the presence of Sc^{3+} as is the case in the absence of Sc^{3+} (Supporting Information, Figures S10 and S11).[49] The overall oxidation

dx.doi.org/10.1021/ic3016723 | Inorg. Chem. 2012, 51, 10025−10036

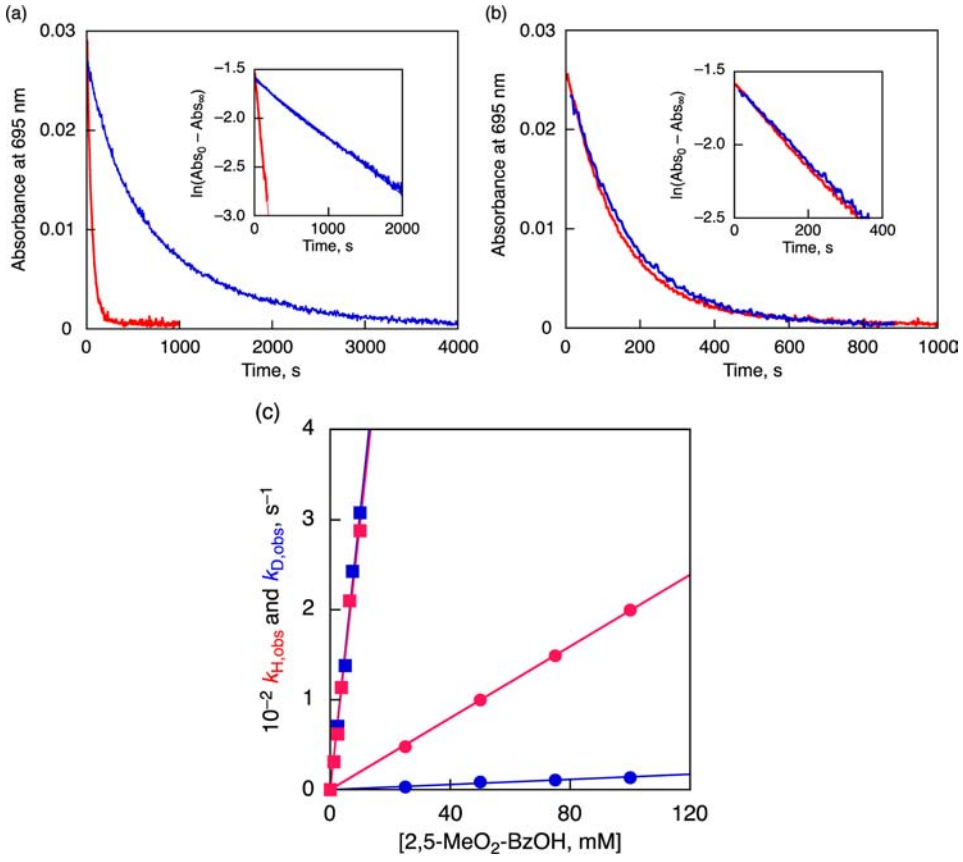

Figure 6. (a) Time courses of the absorption spectral changes observed at 695 nm due to $[Fe^{IV}(O)(N4Py)]^{2+}$ (0.060 mM) in the oxidation of 2,5-$(MeO)_2C_6H_3CH_2OH$ (1.0×10^2 mM) (red) and 2,5-$(MeO)_2C_6H_3CD_2OH$ (1.0×10^2 mM) (blue) in the absence of Sc^{3+}. Inset shows first-order plots of the absorption change at 695 nm. (b) Time courses of the absorption spectral changes observed at 695 nm due to $[Fe^{IV}(O)(N4Py)]^{2+}$ (0.060 mM) in the oxidation of 2,5-$(MeO)_2C_6H_3CH_2OH$ (2.5 mM) (red) and 2,5-$(MeO)_2C_6H_3CD_2OH$ (2.5 mM) (blue) in the presence of Sc^{3+} (2.5 mM). Inset shows first-order plots of the absorption change at 695 nm. (c) Plots of $k_{H,obs}$ (red) and $k_{D,obs}$ (blue) vs [2,5-$(MeO)_2C_6H_3CH_2OH$] and [2,5-$(MeO)_2C_6H_3CD_2OH$] in the absence (circles) and presence (squares) of Sc^{3+} (2.5 mM), respectively.

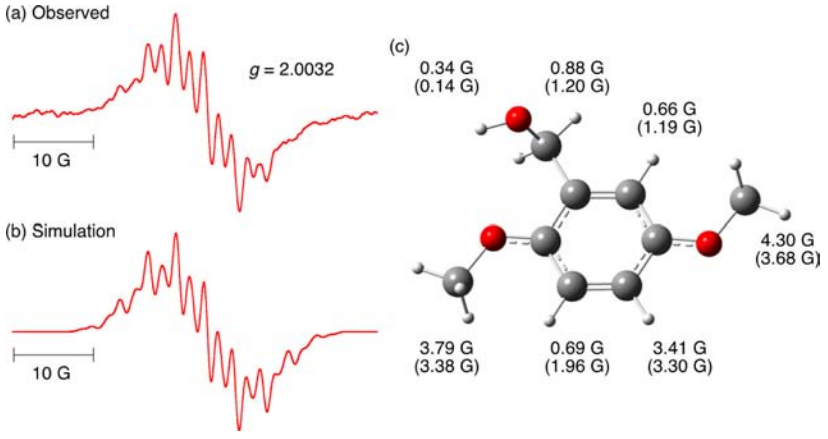

Figure 7. (a) X-band EPR spectrum of 2,5-$(MeO)_2C_6H_3CH_2OH^{\bullet+}$ produced by electron-transfer oxidation of 2,5-$(MeO)_2C_6H_3CH_2OH$ (1.0 mM) by $[Fe^{IV}(O)(N4Py)]^{2+}$ (1.0 mM) in the presence of Sc^{3+} (10 mM) in deaerated MeCN at 298 K. (b) The computer simulation spectrum. (c) DFT optimized structure of 2,5-$(MeO)_2C_6H_3CH_2OH^{\bullet+}$ with hyperfine coupling constants together with the calculated values given in parentheses.

efficiency was determined to be 88% by counting the number of electrons oxidized by $[Fe^{IV}(O)(N4Py)]^{2+}$ ($31 \times 2 + 10 \times 2 + 1 \times 6 = 88$). Because oxidative coupling products were obtained by the oxidation of 2,5-$(MeO)_2C_6H_3CH_2OH$ with one-electron oxidant CAN,[50−52] formation of the dimer products, together with the detection of the radical cation intermediate by absorption and EPR spectra in the oxidation of 2,5-$(MeO)_2C_6H_3CH_2OH$ by $[Fe^{IV}(O)(N4Py)]^{2+}$ in the presence of Sc^{3+} indicates the change of the reaction pathway from the one-step HAT in the absence of Sc^{3+} (step a shown in Scheme 4) to the Sc^{3+}-coupled ET pathway in the presence of Sc^{3+} (step b shown in Scheme 4).[53,54] This is consistent with the bimolecular decay kinetics of 2,5-$(MeO)_2C_6H_3CH_2OH^{\bullet+}$ in Figure 8.

dx.doi.org/10.1021/ic3016723 | Inorg. Chem. 2012, 51, 10025−10036

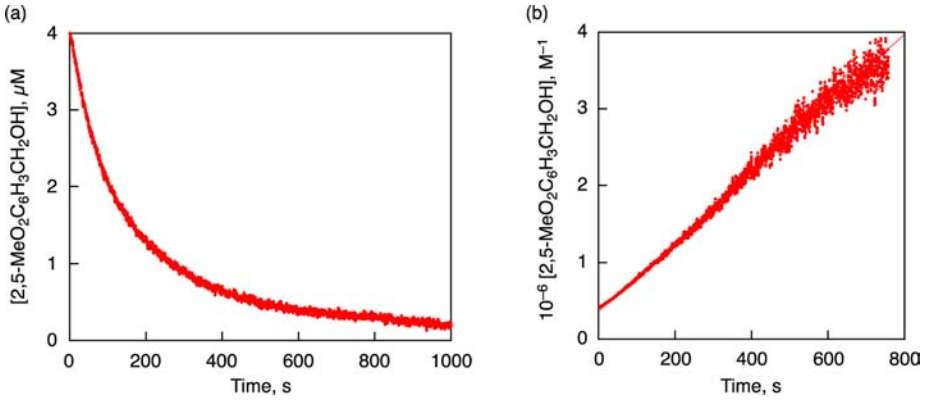

Figure 8. (a) Time course of decay of $[2,5\text{-}(MeO)_2C_6H_3CH_2OH^{\bullet+}]$ observed by EPR measured at 243 K in deaerated MeCN. (b) Second-order plot of the time course of decay in EPR signal of $2,5\text{-}(MeO)_2C_6H_3CH_2OH^{\bullet+}$.

Scheme 3. Proposed Oxidation Pathways for Oxidation of $2,5\text{-}(MeO)_2C_6H_3CH_2OH$ by $[Fe^{IV}(O)(N4Py)]^{2+}$ in the Presence of Sc^{3+}

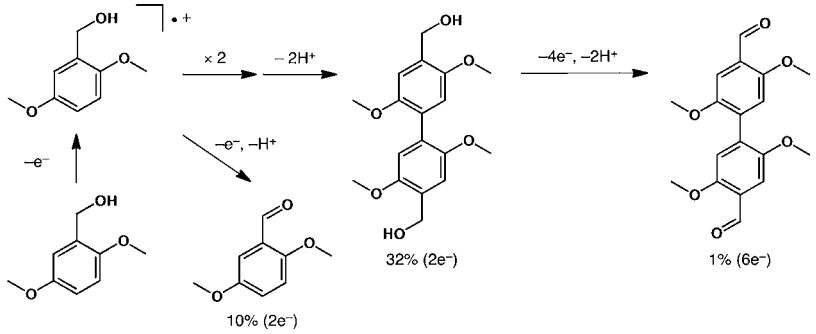

Scheme 4. Reaction Pathway for Oxidation of $2,5\text{-}(MeO)_2C_6H_3CH_2OH$ by $[Fe^{IV}(O)(N4Py)]^{2+}$ in the Absence and Presence of Sc^{3+}

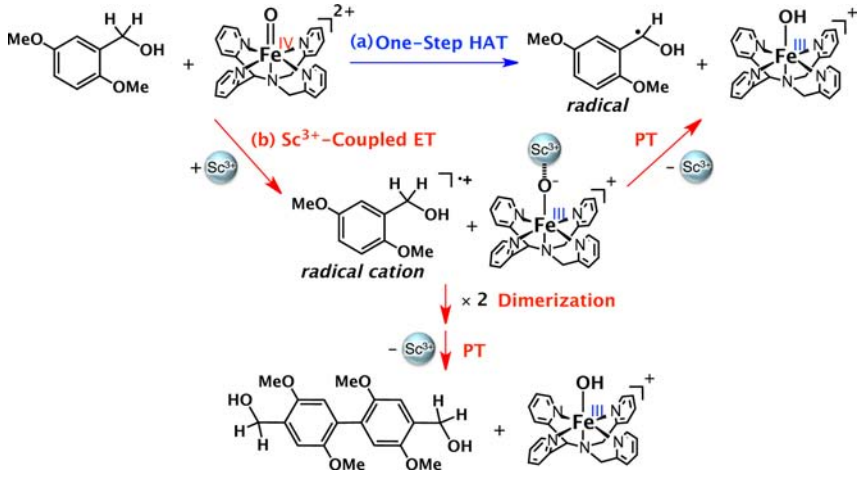

The Sc^{3+}-coupled electron-transfer pathway is further confirmed by the first-order and second-order dependence of k_{ox} of the oxidation of $2,5\text{-}(MeO)_2C_6H_3CH_2OH$ by $[Fe^{IV}(O)(N4Py)]^{2+}$ in the presence of Sc^{3+} on $[Sc^{3+}]$, which is quite similar to that observed Sc^{3+}-coupled ET from $[Fe(bpy)_3]^{2+}$ (one-electron reductant) to $[Fe^{IV}(O)(N4Py)]^{2+}$ on $[Sc^{3+}]$ (Figure 5) and the absence of KIE.

Effect of Sc^{3+} on the Oxidation Rate of Benzyl Alcohol Derivatives by $[Fe^{IV}(O)(N4Py)]^{2+}$. The change in the reaction pathway from one-step HAT to Sc^{3+}-coupled ET may be determined by the one-electron oxidation potentials (E_{ox}) of benzyl alcohol derivatives (see Supporting Information, Table S1 for the E_{ox} values of benzyl alcohol derivatives). To explore the borderline between one-step HAT and Sc^{3+}-coupled ET pathways, we investigated the dependence of the second-order rate constants for the oxidation of a series of benzyl alcohol derivatives on $[Sc^{3+}]$. The results are shown in Figures 9a−9g. The k_{ox} values for the oxidation of benzyl alcohol derivatives with relatively high E_{ox} values, $p\text{-}NO_2C_6H_4CH_2OH$, $C_6H_5CH_2OH$, and $p\text{-}ClC_6H_4CH_2OH$, were the same as those in the absence of Sc^{3+} with increasing concentration of Sc^{3+} (Figures 9a−9c), whereas the k_{ox} values for the oxidation of

dx.doi.org/10.1021/ic3016723 | Inorg. Chem. 2012, 51, 10025−10036

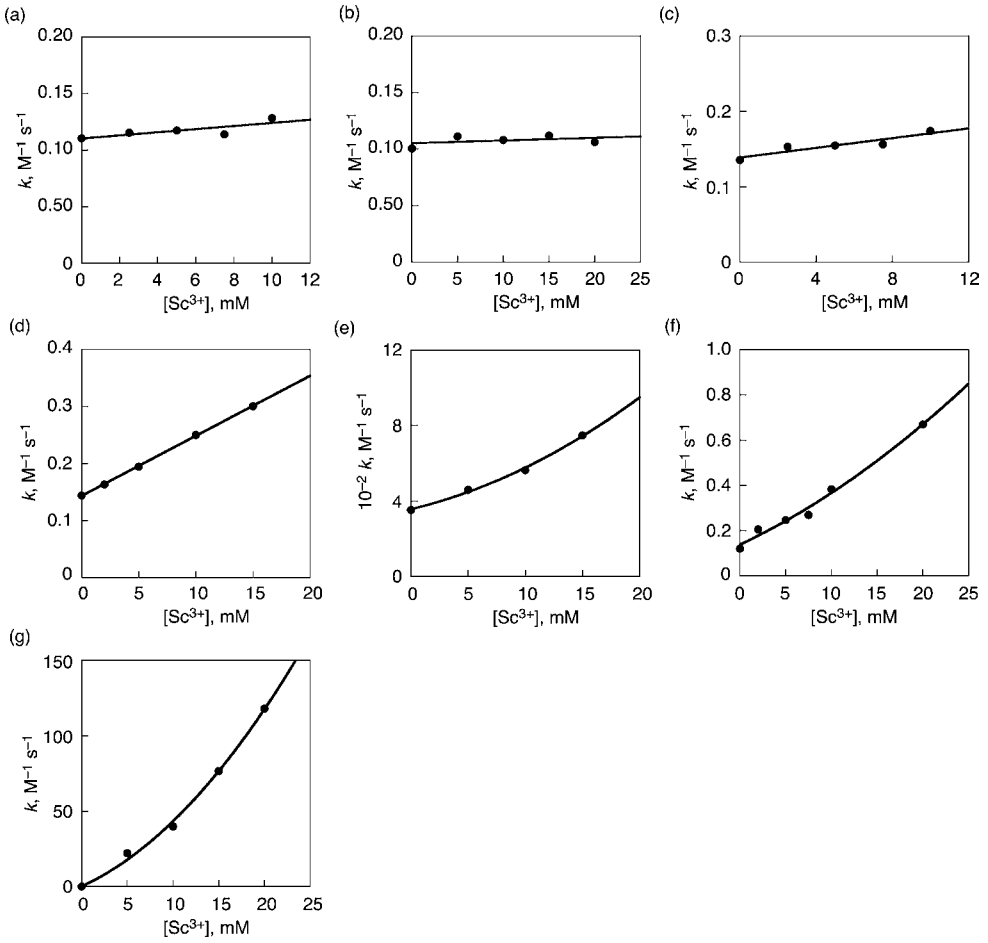

Figure 9. Plots of k_{ox} vs $[Sc^{3+}]$ in the reaction of $[Fe^{IV}(O)(N4Py)]^{2+}$ (0.10 mM) and benzyl alcohol derivatives in the presence of Sc^{3+} in deaerated MeCN at 298 K: (a) *p*-$NO_2C_6H_4CH_2OH$ (25 mM), (b) *p*-$ClC_6H_4CH_2OH$ (50 mM), (c) *p*-$MeC_6H_4CH_2OH$ (25 mM), (d) *p*-$MeOC_6H_4CH_2OH$ (50 mM), (e) $Me_5C_6CH_2OH$ (25 mM), (f) 3,5-$(MeO)_2C_6H_3CH_2OH$ (10 mM), and (g) 3,4,5-$(MeO)_3C_6H_2CH_2OH$ (0.050 mM).

benzyl alcohol derivatives with lower oxidation potentials, *p*-$MeC_6H_4CH_2OH$, *p*-$MeOC_6H_4CH_2OH$, $Me_5C_6CH_2OH$, 3,5-$(MeO)_2C_6H_3CH_2OH$, 3,4,5-$(MeO)_3C_6H_2CH_2OH$, and 2,5-$(MeO)_2C_6H_3CH_2OH$, increased with increasing concentration of Sc^{3+} (Figures 9d–9g) as is the case for the oxidation of 2,5-$(MeO)_2C_6H_3CH_2OH$ (Figure 5). Although no radical cation intermediates were observed in the oxidation of *p*-$MeOC_6H_4CH_2OH$, $Me_5C_6CH_2OH$, 3,5-$(MeO)_2C_6H_3CH_2OH$, and 3,4,5-$(MeO)_3$-$C_6H_2CH_2OH$ in the presence of Sc^{3+} (10 mM), the acceleration may be attributed to Sc^{3+}-coupled ET. The $-\Delta G_{et}$ and k_{ox} values of the oxidation of a series of benzyl alcohol derivatives by $[Fe^{IV}(O)(N4Py)]^{2+}$ in the absence and presence of Sc^{3+} (10 mM) are summarized in Table 1. The $-\Delta G_{et}$ values (in eV) were determined from the E_{ox} values of benzyl alcohol derivatives for the one-electron oxidation to give the corresponding radical cations and the E_{red} values of $[Fe^{IV}(O)(N4Py)]^{2+}$ in the absence and the presence of Sc^{3+} (10 mM) by eq 2, where *e* is the elementary charge.[55]

$$-\Delta G_{et} = e(E_{red} - E_{ox}) \quad (2)$$

Figure 10 shows plots of log k_{ox} of oxidation of benzyl alcohols by $[Fe^{IV}(O)(N4Py)]^{2+}$ in the absence and presence of Sc^{3+} (10 mM) and log k_{et} of electron transfer from one-electron reductants to $[Fe^{IV}(O)(N4Py)]^{2+}$ in the presence of Sc^{3+} (10 mM) vs driving force of ET ($-\Delta G_{et}$). In the absence of Sc^{3+}, the $-\Delta G_{et}$ values are largely negative (endergonic) and the log

Table 1. Driving Force for ET ($-\Delta G_{et}$) and Second-Order Rate Constants (k_{ox}) for Oxidation of Benzyl Alcohol Derivatives with $[Fe^{IV}(O)(N4Py)]^{2+}$ in the Absence and Presence of Sc^{3+} (10 mM) in MeCN at 298 K

		$-\Delta G_{et}$, eV		k_{ox}, M^{-1} s^{-1}	
entry	substituent	Sc^{3+} (0 mM)	Sc^{3+} (10 mM)	Sc^{3+} (0 mM)	Sc^{3+} (10 mM)
1	*p*-NO_2	−2.37	−1.69	1.1×10^{-1}	1.3×10^{-1}
2	*p*-H	−1.82	−1.14	9.9×10^{-2}	9.9×10^{-2}
3	*p*-Cl	−1.74	−1.04	1.0×10^{-1}	1.1×10^{-1}
4	*p*-Me	−1.54	−0.86	1.4×10^{-1}	1.7×10^{-1}
5	Me_5	−1.14	−0.61	3.5×10^{-2}	5.6×10^{-2}
6	*p*-MeO	−1.07	−0.59	1.4×10^{-1}	2.5×10^{-1}
7	3,5-$(MeO)_2$	−0.98	−0.30	1.2×10^{-1}	3.8×10^{-1}
8	3,4,5-$(MeO)_3$	−0.71	−0.23	1.5×10^{-1}	4.0×10
9	2,5-$(MeO)_2$	−0.69	−0.14	2.0×10^{-1}	1.3×10

k_{ox} values are rather independent of the $-\Delta G_{et}$ values (blue points in Figure 10). The log k_{ox} values in the absence of Sc^{3+} are much larger than those predicted by the extrapolated line of electron transfer, indicating that the oxidation of benzyl alcohol derivatives by $[Fe^{IV}(O)(N4Py)]^{2+}$ undergoes via one-step HAT rather than via electron transfer. This is also supported by the

dx.doi.org/10.1021/ic3016723 | *Inorg. Chem.* 2012, 51, 10025–10036

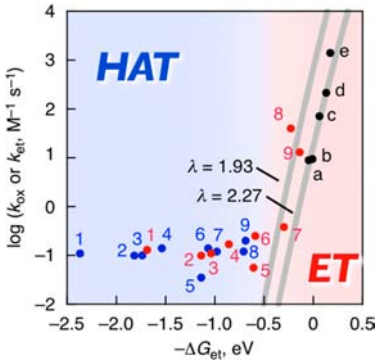

Figure 10. Plots of log k_{ox} for oxidation of benzyl alcohol derivatives (numbers refer to compounds in Table 1) by $[Fe^{IV}(O)(N4Py)]^{2+}$ in MeCN at 298 K vs $-\Delta G_{et}$ for electron transfer from benzyl alcohol derivatives to $[Fe^{IV}(O)(N4Py)]^{2+}$ in the absence (blue) of Sc^{3+} and the presence (red) of Sc^{3+} (10 mM). Black points are plots of log k_{et} of electron transfer from one-electron reductants (a: $[Ru^{II}(bpy)_3]^{2+}$, b: $[Fe^{II}(Clphen)_3]^{2+}$, c: $[Ru^{II}(Me_2bpy)_3]^{2+}$, d: $[Fe^{II}(bpy)_3]^{2+}$, e: $[Fe^{II}(Ph_2phen)_3]^{2+}$) to $[Fe^{IV}(N4Py)(O)]^{2+}$ in the presence of 10 mM of Sc^{3+} in MeCN at 298 K vs $-\Delta G_{et}$. The blue and red parts correspond to HAT and ET pathways, respectively. The solid lines are drawn using eq 4 with λ values of 1.93 and 2.27 eV.

KIE observed in the oxidations of $C_6H_5CD_2OH$ and 2,5-$(MeO)_2C_6H_3CD_2OH$ in the absence of Sc^{3+} (Figure 3).

In sharp contrast to the case in the absence of Sc^{3+}, log k_{ox} values of benzyl alcohol derivatives, which are accelerated by the presence of Sc^{3+} (10 mM) (entries 7−9), show similar driving force dependence to that of log k_{et} of electron transfer from a series of one-electron reductants to $[Fe^{IV}(O)(N4Py)]^{2+}$ in the presence Sc^{3+} (10 mM).[56] Both log k_{ox} and log k_{et} values increase with increasing ET driving force ($-\Delta G_{et}$ values). The ET driving force dependence of k_{et} and k_{ox} is well fitted by the Marcus equation of outer-sphere electron transfer (eq 3), where Z is the frequency factor (1×10^{11} M^{-1} s^{-1}) and λ is the reorganization energy of electron transfer.[57,58] The dependence of log k_{ox} on $-\Delta G_{et}$ clearly indicates the

$$\log k_{ox} = \log Z - \lambda(1 + \Delta G_{et}/\lambda)^2/(2.3 \times 4k_BT) \quad (3)$$

occurrence of Sc^{3+}-coupled ET from benzyl alcohol derivatives to $[Fe^{IV}(O)(N4Py)]^{2+}$. Although the $-\Delta G_{et}$ values for entry 7−9 are negative (endergonic), the Sc^{3+}-coupled ET may be followed by fast subsequent reaction (pathway b in Scheme 4). The λ values for electron transfer from one-electron reductants and benzyl alcohol derivatives to $[Fe^{IV}(O)(N4Py)]^{2+}$ in the presence of 10 mM of Sc^{3+} are determined to be 2.27 and 1.93 eV by fitting plots of entries a−e and 7−9 in red in Figure 10 with eq 3, respectively.

On the other hand, the k_{ox} values of benzyl alcohol derivatives are independent of the ET driving force even in the presence of Sc^{3+} (10 mM) when $-\Delta G_{et}$ is smaller than −0.5 eV (entries 1−4 in Table 1). This indicates that the oxidation of those benzyl alcohol derivatives proceeds via one-step HAT, which is an energetically much more favorable pathway than the highly endergonic Sc^{3+}-coupled ET. The rates of oxidation of benzyl alcohol derivatives (entries 5 and 6 in Table 1) are slightly accelerated by the presence of Sc^{3+} (10 mM) (1.8 and 1.6 times respectively), and the log k_{ox} values are on the borderline of the mechanism change between one-step HAT and Sc^{3+}-coupled ET.[59,60]

The comparison of the driving force dependence of k_{ox} and k_{et} in Figure 10 has provided a clear view with regard to the borderline of the mechanism change between one-step HAT and Sc^{3+}-coupled ET. The results at a different concentration of Sc^{3+} (1.0 mM) are presented in Supporting Information, Figure S14. Although the best fit λ value (2.33 eV) for the driving force dependence of log k_{et} with 1.0 mM Sc^{3+} becomes larger than the value with 10 mM Sc^{3+} (2.27 eV) and therefore the plot looks somewhat different, the conclusion on the mechanism change between one-step HAT and Sc^{3+}-coupled ET remains virtually the same.

It should be noted that it is rather unusual to apply the Marcus theory to conditional rate constants that depend on the concentration of Sc^{3+}. Nevertheless we can explain the dependence of the rate constant on the concentration of Sc^{3+} using the Marcus theory as follows.[58] Under the conditions such that $\lambda \ll -\Delta G_{et}$ in Figure 10, the k_{et} value is estimated by the Marcus cross relationship as shown in eq 4,[57] where k_{Dex}, k_{Aex}, and K_{et} are the rate

$$k_{et} = (k_{Dex}k_{Aex}K_{et})^{1/2} \quad (4)$$

constant of electron exchange between electron donor (D) and the radical cation, the rate constant of electron exchange between electron acceptor (A) and the one-electron reduced species, and the equilibrium constants of the electron transfer from D to A. The k_{Dex} value is constant independent of concentration of Sc^{3+}, whereas k_{Aex} and K_{et} are expected to increase in proportion to $[Sc^{3+}]^2$ at high concentrations of Sc^{3+} as given by eqs 5 and 6, respectively, where k_{Aex0} and K_{et0} are the proportional constants. In such a case, the dependence of k_{et} on

$$k_{Aex} = k_{Aex0}[Sc^{3+}]^2 \quad (5)$$

$$K_{et} = K_{et0}[Sc^{3+}]^2 \quad (6)$$

$[Sc^{3+}]$ is given by eq 7, which agrees with the results in Figure 5.

$$k_{et} = (k_{Dex}k_{Aex0}K_{et0})^{1/2}[Sc^{3+}]^2 \quad (7)$$

The dependence of log k_1 and log k_2 of Sc^{3+}-coupled ET on $-\Delta G_{et}$ in the absence of Sc^{3+} is shown in Supporting Information, Figure S15, where a roughly parallel relationship between k_1 and k_2 is observed. This plot for benzyl alcohol derivatives is not shown because the k_1 and k_2 values of benzyl alcohol derivatives close to the region of one-step HAT could not be obtained accurately because of the large contribution of k_0.

■ CONCLUSION

In this study, we have demonstrated the change of the rate-determining step in the oxidation of benzyl alcohol derivatives by $[Fe^{IV}(O)(N4Py)]^{2+}$ from one-step HAT to Sc^{3+}-coupled ET depending on the one-electron oxidation potentials of benzyl alcohol derivatives. The change in the reaction mechanism is initiated by acceleration of ET by Sc^{3+} while HAT is not accelerated by Sc^{3+} at all.[61] Such a change in the reaction pathways by the presence of Sc^{3+} has been clearly shown by the disappearance of KIE in the presence of Sc^{3+} in contrast to a large KIE value observed in the absence of Sc^{3+}, when formation of the radical cation of a benzyl alcohol derivative was detected as the initial product of Sc^{3+}-coupled ET from the substrate to $[Fe^{IV}(O)(N4Py)]^{2+}$, leading to the dimerized product as a major product in contrast to the corresponding aldehyde obtained as the sole product in the absence of Sc^{3+}.

dx.doi.org/10.1021/ic3016723 | Inorg. Chem. 2012, 51, 10025−10036

The mechanistic borderline between one-step HAT and Sc^{3+}-coupled ET has been found to be determined by the ET driving force from the substrate to $[Fe^{IV}(O)(N4Py)]^{2+}$ with the borderline of $-\Delta G_{et} \approx -0.5$ eV. The C−H bond is cleaved via HAT when $-\Delta G_{et}$ is more negative than −0.5 eV, whereas Sc^{3+}-coupled ET becomes a predominant pathway when $-\Delta G_{et}$ is more positive than −0.5 eV. In other words, Sc^{3+}-coupled ET occurs when E_{ox} of substrate is more negative than 1.7 V. This study provides the first example for the change in the mechanism of oxidation of substrates by a high-valent metal-oxo complex from one-step HAT to ET that is accelerated by Sc^{3+} depending on the ET driving force. The oxidation reaction takes place even when $-\Delta G_{et}$ is negative, that is, ET is endergonic, indicating the ET process is coupled with the following proton transfer. It is of interest to note that the borderline between one-step HAT and Sc^{3+}-coupled ET is at the ET driving force (ΔG_{et}) of about −0.5 eV, which is similar to that reported previously for the borderline between one-step oxygen atom transfer and Sc^{3+}-coupled ET.[57] This type of switching in reaction pathway from HAT to ET depending on the $-\Delta G_{et}$ value would generally appear in the reaction systems where high-valent oxometal species are employed as an oxidant such as compound I or MnO_4^-, especially in oxidation of substrates with relatively low oxidation potential or in the presence of acids which shift one-electron reduction potential of metal-oxo species positively.

■ ASSOCIATED CONTENT

Supporting Information

Further details are given in Table S1 and Figures S1−S13. This material is available free of charge via the Internet at http://pubs.acs.org.

■ AUTHOR INFORMATION

Corresponding Author

*E-mail: fukuzumi@chem.eng.osaka-u.ac.jp (S.F.), wwnam@ewha.ac.kr (W.N.).

Notes

The authors declare no competing financial interest.

■ ACKNOWLEDGMENTS

This work at OU was supported by a Grant-in-Aid (No 20108010 to S.F.) and a Global COE program, "the Global Education and Research Center for Bio-Environmental Chemistry" from MEXT, Japan (to S.F.), the work at EWU was supported by NRF/MEST of Korea through CRI (to W.N.), GRL (2010-00353) (to W.N.), and WCU (R31-2008-000-10010-0) (to W.N. and S.F.). Y.M. appreciates support from the Global COE program of Osaka University and Grant-in-Aid for JSPS fellowship for young scientists.

■ REFERENCES

(1) (a) Kochi, J. K., Ed.; *Free Radicals*; Wiley: New York, 1973. (b) Olah, G. A.; Molnár, Á. *Hydrocarbon Chemistry*; Wiley: New York, 1995. (c) Larock, R. C. *Comprehensive Organic: A Guide to Functional Group Preparations*; Wiley-VCH: New York, 1999. (d) Halliwell, B.; Gutteridge, J. M. C. *Free Radicals in Biology and Medicine*; Oxford University Press: Oxford, U.K., 2007. (e) Hynes, J. T., Klinman, J. P., Limbach, H.-H., Schowen, R. L., Eds.; *Hydrogen-Transfer Reactions: Biological Aspects I-II*; Wiley-VCH: Weinheim, Germany, 2007; Vol. 3.

(2) (a) Stewart, R. *Oxidation Mechanisms*; Benjamin: New York, 1964. (b) Mijs, W. J.; De Jonge, C. R. H. I. *Organic Synthesis by Oxidation with Metal Compounds*; Plenum: New York, 1986.

(3) (a) Roithová, J.; Schröder, D. *Chem. Rev.* **2010**, *110*, 1170. (b) Chiesa, M.; Giamello, E.; Che, M. *Chem. Rev.* **2010**, *110*, 1320. (c) Ding, X.-L.; Wu, X.-N.; Zhao, Y.-X.; He, S.-G. *Acc. Chem. Res.* **2012**, *45*, 382. (d) Dietl, N.; Schlangen, M.; Schwarz, H. *Angew. Chem., Int. Ed.* **2012**, *51*, 2.

(4) (a) Penner-Hahn, J. E.; Eble, K. S.; McMurry, T. J.; Renner, M.; Balch, A. L.; Groves, J. T.; Dawson, J. H.; Hodgson, K. O. *J. Am. Chem. Soc.* **1986**, *108*, 7819. (b) Schlichting, I.; Berendzen, J.; Chu, K.; Stock, A. M.; Maves, S. A.; Benson, D. E.; Sweet, R. M.; Ringe, D.; Petsko, G. A.; Sligar, S. G. *Science* **2000**, *287*, 1615. (c) Green, M. T.; Dawson, J. H.; Gray, H. B. *Science* **2004**, *304*, 1653. (d) Rittle, J.; Green, M. T. *Science* **2011**, *330*, 933. (e) Dunford, H. B. *Heme Peroxidases*; Wiley-VCH: New York, 1999. (f) Ortiz de Montellano, P. R. *Cytochrome P450: Structure, Mechanism, and Biochemistry*, 3rd ed.; Kluwer Academic/Plenum Publishers: New York, 2005.

(5) (a) Sono, M.; Roach, M. P.; Coulter, E. D.; Dawson, J. H. *Chem. Rev.* **1996**, *96*, 2841. (b) Harris, D. L.; Loew, G. H. *J. Am. Chem. Soc.* **1998**, *120*, 8941. (c) Newcomb, M.; Shen, R.; Choi, S.-Y.; Toy, P. H.; Hollenberg, P. F.; Vaz, A. D. N.; Coon, M. J. *J. Am. Chem. Soc.* **2000**, *122*, 2677. (d) Ortiz de Montellano, P. R. *Chem. Rev.* **2010**, *110*, 932.

(6) (a) Elkins, J. M.; Ryle, M. J.; Clifton, I. J.; Hotopp, J. C. D.; Lloyd, J. S.; Burzlaff, N. I.; Baldwin, J. E.; Hausinger, R. P.; Roach, P. L. *Biochemistry* **2002**, *41*, 5185. (b) Price, J. C.; Barr, E. W.; Glass, T. E.; Krebs, C.; Bollinger, J. M., Jr. *J. Am. Chem. Soc.* **2003**, *125*, 13008. (c) Price, J. C.; Barr, E. W.; Tirupati, B.; Krebs, C.; Bollinger, J. M., Jr. *Biochemistry* **2003**, *42*, 7497. (d) Proshlyakov, D. A.; Henshaw, T. F.; Monterosso, G. R.; Ryle, M. J.; Hausinger, R. P. *J. Am. Chem. Soc.* **2004**, *126*, 1022. (e) Price, J. C.; Barr, E. W.; Hoffart, L. M.; Krebs, C.; Bollinger, J. M., Jr. *Biochemistry* **2005**, *44*, 8138.

(7) (a) Ekstrom, G.; Norsten, C.; Cronholm, T.; Ingelman-Sundberg, M. *Biochemistry* **1987**, *26*, 7348. (b) Vaz, A. D. N.; Coon, M. J. *Biochemistry* **1994**, *33*, 6442. (c) Guengerich, F. P. *Chem. Res. Toxicol.* **2001**, *14*, 611. (d) Kroutil, W.; Mang, H.; Edegger, K.; Faber, K. *Adv. Synth. Catal.* **2004**, *346*, 125.

(8) (a) Rettie, A. E.; Rettenmeier, A. W.; Howald, W. N.; Baillie, T. A. *Science* **1987**, *235*, 890. (b) Rettie, A. E.; Boberg, M.; Rettenmeier, A. W.; Baillie, T. A. *J. Biol. Chem.* **1988**, *263*, 13733. (c) Giner, J. L.; Silva, C. J.; Djerassi, C. *J. Am. Chem. Soc.* **1990**, *112*, 9626. (d) Collins, J. R.; Camper, D. L.; Loew, G. H. *J. Am. Chem. Soc.* **1991**, *113*, 2736. (e) Buist, P. H.; Marecak, D. M. *J. Am. Chem. Soc.* **1992**, *114*, 5073.

(9) (a) Baldwin, J. E.; Schofield, C. *Chemistry of β-Lactams*; Blackie: Glasgow, U.K., 1992. (b) Roach, P. L.; Clifton, I. J.; Hensgens, C. M. H.; Shibata, N.; Schofield, C. J.; Hajdu, J.; Baldwin, J. E. *Nature* **1997**, *387*, 827. (c) Brown, C. D.; Neidig, M. L.; Neibergall, M. B.; Lipscomb, J. D.; Solomon, E. I. *J. Am. Chem. Soc.* **2007**, *129*, 7427.

(10) (a) Krebs, C.; Fujimori, D. G.; Walsh, C. T.; Bollinger, J. M., Jr. *Acc. Chem. Res.* **2007**, *40*, 484. (b) Galonić, D. P.; Barr, E. W.; Walsh, C. T.; Bollinger, J. M., Jr.; Krebs, C. *Nat. Chem. Biol.* **2007**, *3*, 113.

(11) Warren, J. J.; Tronic, T. A.; Mayer, J. M. *Chem. Rev.* **2010**, *110*, 6961.

(12) (a) Balcells, D.; Clot, E.; Eisenstein, O. *Chem. Rev.* **2010**, *110*, 749. (b) Gunay, A.; Theopold, K. H. *Chem. Rev.* **2010**, *110*, 1060.

(13) (a) MacBeth, C. E.; Golombek, A. P.; Young, V. G., Jr.; Yang, C.; Kuczera, K.; Hendrich, M. P.; Borovik, A. S. *Science* **2000**, *289*, 938. (b) Rohde, J.-U.; In, J.-H.; Lim, M. H.; Brennessel, W. W.; Bukowski, M. R.; Stubna, A.; Münck, E.; Nam, W.; Que, L., Jr. *Science* **2003**, *299*, 1037. (c) Que, L., Jr.; Ho, R. Y. N. *Chem. Rev.* **1996**, *96*, 2607. (d) Solomon, E. S.; Brunold, T. C.; Davis, M. I.; Kemsley, J. N.; Lee, S.-K.; Lehnert, N.; Neese, F.; Skulan, A. J.; Yang, Y.-S.; Zhou, J. *Chem. Rev.* **2000**, *100*, 235. (e) Que, L., Jr. *Acc. Chem. Res.* **2007**, *40*, 493. (f) Nam, W. *Acc. Chem. Res.* **2007**, *40*, 522. (g) Hohenberger, J.; Ray, K.; Meyer, K. *Nat. Commun.* **2012**, *3*, 720. (h) de Visser, S. P.; Rohde, J.-U.; Lee, Y.-M.; Cho, J.; Nam, W. *Coord. Chem. Rev.* **2012**, DOI: 10.1016/j.ccr.2012.06.002.

(14) (a) Groves, J. T.; Haushalter, R. C.; Nakamura, M.; Nemo, T. E.; Evans, B. J. *J. Am. Chem. Soc.* **1981**, *103*, 2884. (b) Meunier, B. *Chem. Rev.* **1992**, *92*, 1411. (c) Sheldon, R. A. *Metalloprophyrins in Catalytic Oxidations*; Marcel Dekker: New York, 1994. (d) Meunier, B., Ed. *Metal-Oxo and Metal-Peroxo Species in Catalytic Oxidations*;

Springer-Verlag: Berlin, Germany, 2000. (e) Shaik, S.; Cohen, S.; Wang, Y.; Chen, H.; Kumar, D.; Thiel, W. *Chem. Rev.* **2010**, *110*, 949.
(15) Lubben, M.; Meetsma, A.; Wilkinson, E. C.; Feringa, B.; Que, L., Jr. *Angew. Chem., Int. Ed.* **1995**, *34*, 1512.
(16) (a) Kaizer, J.; Klinker, E. J.; Oh, N. Y.; Rohde, J.-U.; Song, W. J.; Stubna, A.; Kim, J.; Münck, E.; Nam, W.; Que, L., Jr. *J. Am. Chem. Soc.* **2004**, *126*, 472. (b) Kumar, D.; Hirao, H.; Que, L., Jr.; Shaik, S. *J. Am. Chem. Soc.* **2005**, *127*, 8026. (c) Wang, D.; Zhang, M.; Bühlmann, P. B.; Que, L., Jr. *J. Am. Chem. Soc.* **2010**, *132*, 7638.
(17) Oh, N. Y.; Suh, Y.; Park, M. J.; Seo, M. S.; Kim, J.; Nam, W. *Angew. Chem., Int. Ed.* **2005**, *44*, 4235.
(18) (a) Gupta, R.; Borovik, A. S. *J. Am. Chem. Soc.* **2003**, *125*, 13234. (b) Pestovsky, O.; Bakac, A. *J. Am. Chem. Soc.* **2004**, *126*, 13757. (c) Lam, W. W. Y.; Man, W.-L.; Lau, T.-C. *Coord. Chem. Rev.* **2007**, *251*, 2238. (d) de Visser, S. P. *J. Am. Chem. Soc.* **2010**, *132*, 1087. (e) Prokop, K. A.; de Visser, S. P.; Goldberg, D. P. *Angew. Chem., Int. Ed.* **2010**, *49*, 5091. (f) Kojima, T.; Nakayama, K.; Ikemura, K.; Ogura, T.; Fukuzumi, S. *J. Am. Chem. Soc.* **2011**, *133*, 11692.
(19) (a) Mayer, J. M. *Acc. Chem. Res.* **1998**, *31*, 441. (b) Cukier, R. I.; Nocera, D. G. *Annu. Rev. Phys. Chem.* **1998**, *49*, 337. (c) Mayer, J. M. *Annu. Rev. Phys. Chem.* **2004**, *55*, 363. (d) Huynh, M. H. V.; Meyer, T. J. *Chem. Rev.* **2007**, *107*, 5004. (e) Mayer, J. M. *Acc. Chem. Res.* **2011**, *44*, 36.
(20) (a) Goto, Y.; Watanabe, Y.; Fukuzumi, S.; Jones, J. P.; Dinnocenzo, J. P. *J. Am. Chem. Soc.* **1998**, *120*, 10762. (b) Goto, Y.; Matsui, T.; Ozaki, S.; Watanabe, Y.; Fukuzumi, S. *J. Am. Chem. Soc.* **1999**, *121*, 9497. (c) Nehru, K.; Seo, M. S.; Kim, J.; Nam, W. *Inorg. Chem.* **2007**, *46*, 293.
(21) Yuasa, J.; Fukuzumi, S. *J. Am. Chem. Soc.* **2006**, *128*, 14281.
(22) Yuasa, J.; Yamada, S.; Fukuzumi, S. *J. Am. Chem. Soc.* **2006**, *128*, 14938.
(23) For other metal ion-promoted reactions, see: (a) Fukuzumi, S.; Ohkubo, K.; Morimoto, Y. *Phys. Chem. Chem. Phys.* **2012**, *14*, 8472. (b) Fukuzumi, S.; Ohkubo, K.; Okamoto, T. *J. Am. Chem. Soc.* **2002**, *124*, 14147. (c) Fukuzumi, S.; Fujii, Y.; Suenobu, T. *J. Am. Chem. Soc.* **2001**, *123*, 10191. (d) Fukuzumi, S. *Bull. Chem. Soc. Jpn.* **1997**, *70*, 1. (e) Fukuzumi, S.; Okamoto, T. *J. Am. Chem. Soc.* **1993**, *115*, 11600. (f) Fukuzumi, S.; Koumitsu, S.; Hironaka, K.; Tanaka, T. *J. Am. Chem. Soc.* **1987**, *109*, 305. (g) Fukuzumi, S.; Nishizawa, N.; Tanaka, T. *J. Chem. Soc., Perkin Trans. 2* **1985**, 371. (h) Fukuzumi, S.; Kuroda, S.; Tanaka, T. *J. Am. Chem. Soc.* **1985**, *107*, 3020.
(24) (a) Abu-Omar, M. M. *J. Am. Chem. Soc.* **2007**, *129*, 11505. (b) Shearer, J.; Zhang, C. X.; Hatcher, L. Q.; Karlin, K. D. *J. Am. Chem. Soc.* **2003**, *125*, 12670.
(25) There has been no example of C–H bond cleavage that proceeds via a PT/ET pathway, however that of O–H bond cleavage via a PT/ET pathway has been reported. See: Litwinienko, G.; Ingold, K. U. *Acc. Chem. Res.* **2007**, *40*, 222.
(26) (a) Lee, Y.-M.; Kotani, H.; Suenobu, T.; Nam, W.; Fukuzumi, S. *J. Am. Chem. Soc.* **2008**, *130*, 434. (b) Fukuzumi, S.; Kotani, H.; Suenobu, T.; Hong, S.; Lee, Y.-M.; Nam, W. *Chem.—Eur. J.* **2010**, *16*, 354.
(27) (a) Morimoto, M.; Kotani, H.; Park, J.; Lee, Y.-M.; Nam, W.; Fukuzumi, S. *J. Am. Chem. Soc.* **2011**, *133*, 403. (b) Fukuzumi, S. *Prog. Inorg. Chem.* **2009**, *56*, 49.
(28) For the crystal structure of a Sc^{3+}-bound iron(IV)-oxo complex, see: Fukuzumi, S.; Morimoto, Y.; Kotani, H.; Naumov, P.; Lee, Y.-M.; Nam, W. *Nature Chem.* **2010**, *2*, 756.
(29) Sc^{3+} ion is known to be the most effective for metal ion-coupled electron transfer. See: (a) Fukuzumi, S.; Ohkubo, K. *Chem.—Eur. J.* **2000**, *6*, 4532. (b) Fukuzumi, S.; Ohkubo, K. *J. Am. Chem. Soc.* **2002**, *124*, 10270.
(30) For the effect of Brønsted acid on the reactivity of the iron(IV)-oxo complex, see: Park, J.; Morimoto, Y.; Lee, Y.-M.; Nam., W.; Fukuzumi, S. *J. Am. Chem. Soc.* **2012**, *134*, 3903.
(31) Armarego, W. L. F.; Chai, C. L. L. *Purification of Laboratory Chemicals*, 6th ed.; Pergamon Press: Oxford, U.K., 2009.
(32) Saltzman, H., Sharefkin, J. G., Eds.; *Organic Syntheses*, Vol. *V*; Wiley: New York, 1973; p 658.
(33) Tsai, S.-C.; Klinman, J. P. *Biochemistry* **2001**, *40*, 2303.
(34) Mann, C. K.; Barnes, K. K. *Electrochemical Reactions in Non-aqueous Systems*; Marcel Dekker: New York, 1970.
(35) Becke, A. D. *J. Chem. Phys.* **1993**, *98*, 5648.
(36) *Gaussian 09*, Revision A.02; Gaussian, Inc.: Wallingford, CT, 2004.
(37) Dennington, R., II; Keith, T.; Millam, J.; Eppinnett, K.; Hovell, W. L.; Gilliland, R. *Gaussview*; Semichem, Inc.: Shawnee Mission, KS, 2003.
(38) The EPR signals assigned as an alkoxo complex are similar to $[Fe(OMe)(N4Py)]^{2+}$. See: Roelfes, G.; Lubben, M.; Chen, K.; Ho, R. Y. N.; Meetsma, A.; Genseberger, S.; Hermant, R. M.; Hage, R.; Mandal, S. K.; Young, V. G.; Zang, Y.; Kooijman, H.; Spek, A. L.; Que, L., Jr.; Feringa, B. L. *Inorg. Chem.* **1999**, *38*, 1929.
(39) Hong, S.; Lee, Y.-M.; Shin, W.; Fukuzumi, S.; Nam, W. *J. Am. Chem. Soc.* **2009**, *131*, 13910.
(40) The KIE value for this reaction performed at 298 K in the absence of Sc^{3+} is determined to be 13.
(41) There is another possibility that $[Fe^{III}(OH)(N4Py)]^{2+}$ oxidizes $2,5\text{-}(MeO)_2C_6H_3CHOH^{\bullet}$ to yield $[Fe^{II}(N4Py)]^{2+}$, H_2O, and $2,5\text{-}(MeO)_2C_6H_3CHO$. Then, $[Fe^{II}(N4Py)]^{2+}$ is oxidized by $[Fe^{IV}(O)(N4Py)]^{2+}$ to yield $2,5\text{-}(MeO)_2C_6H_3CHO$ and $[Fe^{III}(OH)(N4Py)]^{2+}$. However, a control experiment shows that $[Fe^{IV}(O)(N4Py)]^{2+}$ does not oxidize $[Fe^{II}(N4Py)]^{2+}$ in the presence of $2,5\text{-}(MeO)_2C_6H_3CH_2OH$ in MeCN. Thus, the proportionation of the iron(IV) and iron(II) complexes as a reason why $[Fe^{IV}(O)(N4Py)]^{2+}$ acts as a one-electron oxidant rather than a two-electron oxidant is unlikely under the present reaction conditions.
(42) (a) Atkinson, J. K.; Hollenberg, P. F.; Ingold, K. U.; Johnson, C. C.; Le Tadic, M.-H.; Newcomb, M.; Putt, D. A. *Biochemistry* **1994**, *33*, 10630. (b) Matsuo, T.; Mayer, J. M. *Inorg. Chem.* **2005**, *44*, 2150.
(43) Melander, L.; Saunders, W. H., Jr. *Reaction Rates of Isotopic Molecules*; Wiley Interscience: New York, 1980; pp 29–36.
(44) Klinker, E. J.; Shaik., S.; Hirao, H.; Que, L., Jr. *Angew. Chem., Int. Ed.* **2009**, *48*, 1291.
(45) (a) Lehnert, N.; Solomon, E. I. *J. Biol. Inorg. Chem.* **2003**, *8*, 294. (b) Hatcher, E.; Soudackov, A. V.; Hammes-Schiffer, S. *J. Am. Chem. Soc.* **2004**, *126*, 5763. (c) Meyer, M. P.; Klinman, J. P. *J. Am. Chem. Soc.* **2011**, *133*, 430.
(46) For $2,5\text{-}(MeO)_2C_6H_3OH^{\bullet+}$ produced by photochemical methods, see: (a) Branchi, B.; Bietti, M.; Ercolani, G.; Izquierdo, M. A.; Miranda, M. A.; Stella, L. *J. Org. Chem.* **2004**, *69*, 8874. (b) Baciocchi, E.; Bietti, M.; Gerini, M. F.; Manduchi, L.; Salamone, M.; Steenken, S. *Chem.—Eur. J.* **2001**, *7*, 1408.
(47) The extrapolation of the second-order plot to the time when the reaction was started by mixing two reactant solutions, which is about 5 min before starting EPR measurements, suggests that the radical cation is produced quantitatively.
(48) Yield = $[Product]/[2,5\text{-}(MeO)_2C_6H_3CH_2OH]_0 \times 100$ where $[2,5\text{-}(MeO)_2C_6H_3CH_2OH]_0$ is the initial concentration of $2,5\text{-}(MeO)_2C_6H_3CH_2OH$.
(49) We could not observe the Sc^{3+}-bound complexes by ESI-mass except for $[Fe^{III}(N4Py)(NCMe)]^{3+}$ which may be due to weak Fe-O bond of the Sc^{3+}-bound complex. However, the EPR spectrum of resulting solution shown in Supporting Information, Figure S11b agreed with the spectrum of the Sc^{3+}-bound complex reported in our previous study.[27a]
(50) Love, B. E.; Bonner-Stewart, J.; Forrest, L. A. *Synlett* **2009**, *5*, 813.
(51) The major product in the oxidation of $2,5\text{-}(MeO)_2C_6H_3CH_2OH$ by CAN is not a dimer of aldehyde but diquinone, 4,4′-dimethoxy-[bi-1,4-cyclohexadien-1-yl]-3,3′,6,6′-tetrone.[50]
(52) In the oxidation of benzyl alcohol by $[Fe(O)(N4Py)]^{2+}$ both in the presence and absence of Sc^{3+}, we cannot detect dimerized products as shown in Supporting Information, Figure S2. This may be because the hydrogen-abstracted radicals by $[Fe(O)(N4Py)]^{2+}$ can not produce dimerized products not like radical cations of substrates.

(53) In the oxidation of 2,5-$(MeO)_2C_6H_3CH_2OH$ by $[Ru^{III}(bpy)_3]^{2+}$, no aldehyde formation was observed as a product. This indicates that $[Fe^{III}(O)(N4Py)]^{2+}$–Sc^{3+} works as a base to accept a proton released from 2,5-$(MeO)_2C_6H_3CH_2OH^{\bullet+}$ to produce 2,5-$(MeO)_2C_6H_3CHO$.
(54) The pseudo-first-order rate constants were proportional to concentrations of substrates without exhibiting no intercepts as shown in Figure 6. This indicates that the rate-determining step is the Sc^{3+}-coupled electron transfer followed by subsequent reactions which are faster than the back electron-transfer reaction.
(55) Some of benzyl alcohol derivatives interact with Sc^{3+}. This interaction resulted in the positive shifts of the one-electron oxidation potentials (Supporting Information, Table S1).
(56) The observed rate constant (k_{ox}) consists of three rate constants, i.e., k_0, k_1, and k_2 (eq 1). Under the conditions in Figure 5 ($[Sc^{3+}]$ = 10 mM), k_2 is the main component. Thus, k_{ox} in Figure 10 virtually corresponds to the rate constant for elementary step electron transfer to $[Fe^{IV}(O)(N4Py)]^{2+}$-$(Sc^{3+})_2$.[27a]
(57) (a) Marcus, R. A. *Annu. Rev. Phys. Chem.* **1964**, *15*, 155. (b) Marcus, R. A. *Angew. Chem., Int. Ed. Engl.* **1993**, *32*, 1111.
(58) The Marcus equation can be applied at different concentrations of Sc^{3+}, when the driving force and reorganization energy of electron transfer are changed as discussed previously on metal ion-coupled electron transfer; see: Okamoto, K.; Imahori, H.; Fukuzumi, S. *J. Am. Chem. Soc.* **2003**, *125*, 7014.
(59) For the use of the Marcus plot to clarify the reaction mechanisms of $[Fe^{IV}(O)(N4Py)]^{2+}$, see: (a) Park, J.; Morimoto, Y.; Lee, Y.-M.; Nam, W.; Fukuzumi, S. *J. Am. Chem. Soc.* **2011**, *133*, 5236. (b) Park, J.; Morimoto, Y.; Lee, Y.-M.; You, Y.; Nam, W.; Fukuzumi, S. *Inorg. Chem.* **2011**, *50*, 11612.
(60) No clear correlation between log k_{ox} values and bond dissociation energies ($BDE_{(C-H)}$) of C–H bonds at the benzyl position of a series of benzyl alcohol derivatives calculated with DFT excludes the possibility that the reaction pathway is controlled by $BDE_{(C-H)}$ (Supporting Information, Figure S13).
(61) The binding of Sc^{3+} to $[Fe^{IV}(O)(N4Py)]^{2+}$ may increase the oxidizing ability. However, the direct hydrogen atom transfer reaction may be prohibited by the steric effect of Sc^{3+}. In contrast to this, electron transfer is generally insensitive to the steric effect because outer-sphere electron transfer requires little interaction between electron donor and acceptor molecules. This is the reason why ET is accelerated whereas no acceleration of HAT occurs by the addition of Sc^{3+}.